Degradable particulate composite reinforced with nanofibres for biomedical applications

E.D. Pinho, A. Martins, J.V. Araújo, R.L. Reis, N.M. Neves [*]

3B's Research Group—Biomaterials, Biodegradables and Biomimetics, University of Minho,
Headquarters of the European Institute of Excellence on
Tissue Engineering and Regenerative Medicine, AvePark, 4806-909 Taipas, Guimarães, Portugal
IBB—Institute for Biotechnology and Bioengineering, PT Associated Laboratory, Guimarães, Portugal

Abstract

Nanofibre-based structures and their composites are increasingly being studied for many biomedical applications, including tissue engineering scaffolds. These materials enable architectures resembling the extracellular matrix to be obtained. The search for optimized supports and carriers of cells is still a major challenge for the tissue engineering field. The main purpose of this work is to develop a novel composite structure that combines microparticles and nanofibres in reinforced polymeric microfibres. This innovative combination of materials is obtained by melting extrusion of a particulate composite reinforced with chitosan nanofibre meshes (0.05 wt.%) produced by the electrospinning technique. The reinforced microfibres were analysed by scanning electron microscopy and showed a considerable alignment of the chitosan nanofibres along the longitudinal main axis of the microfibre composite structure. The tensile mechanical properties revealed that the introduction of the nanofibre reinforcement in the particulate microfibre composite increased the tensile modulus by up to 70%. The various structures were subjected to swelling and degradation tests immersed in an isotonic saline solution at 37 °C. The presence of chitosan nanofibres in the particulate microfibres enhances the water uptake by up to 24%. The combination of good mechanical properties and enhanced degradability of the developed structures is believed to have great potential for various biomedical applications, including three-dimensional fibre mesh scaffolds to be applied in the field of bone tissue engineering.
© 2008 Acta Materialia Inc. Published by Elsevier Ltd. All rights reserved.

Keywords: Biodegradable materials; Biomaterials; Nanofibres; Polymeric composite; Tissue engineering

1. Introduction

The extracellular matrix (ECM) of connective tissues is a biological example of a fibrous structure based in collagen fibrils reinforced by other fibrous structures such as glycosaminoglycans and polysaccharides. Collagen fibre, being the primary structural element of the ECM of many tissues, provides a target for the design of new fibrous structures intended for tissue engineering scaffolding. Type I collagen molecules assemble into triple helix collagen fibrils which are long filamentous structures organized to form collagen fibrils and hierarchically aligned in overlapped bundles (each fibril may have more than 700 individual collagen protein strands) [1]. The precise spatial organization of collagen structures in vivo determines the properties of the tissues, such as the tensile strength. In the case of bone, entire collagen triple helices lie in a parallel staggered array to ensure continuity to its structure. Bone is an outstanding structural tissue and a true nano-composite reinforced by the HAp crystals. It is a complex and highly specialized connective tissue that constitutes the skeleton of the vertebrates [2]. Structurally, bone is organized and assembled in various levels of hierarchical

---

[*] Corresponding author. Address: 3B's Research Group—Biomaterials, Biodegradables and Biomimetics, University of Minho, Headquarters of the European Institute of Excellence on Tissue Engineering and Regenerative Medicine, AvePark, 4806-909 Taipas, Guimarães, Portugal. Tel.: +351 253510905; fax: +351 253 604498.

E-mail address: nuno@dep.uminho.pt (N.M. Neves).

units elegantly designed at several length scales, nano to macro, to ensure its multiple functions. The structure of bone inspired the authors to develop the ternary composites proposed in the present paper.

Generally, the collagen fibrils in bone are 50–500 nm in diameter and can be hundreds of micrometres long. In native tissues, these fibrils are further assembled into larger collagen bundles that may be several micrometres in diameter and millimetres to centimetres in length [3]. The anisotropic fibril architecture of natural ECM has important implications on the cell behaviour [4]. These collagen assemblies are characterized by high stiffness and tensile strength, which imparts resistance to compression, tensile and shear loads to the tissues [5]. It is therefore advantageous to engineer tissues consisting of organized fibres to exploit these physiological and mechanical cues [6].

One of the most important requirements for a nanofibre-reinforced composite is that the external stresses applied are efficiently transferred to the nanofibres, allowing them to take a disproportionate share of the load. If the interface properties are adequate and the fibre distribution is homogeneous, the shear stresses developing at the interface of each nanofibre will support the stress applied to the composite [7]. An efficient composite requires that the nanofibres be uniformly dispersed as isolated nanofibres and individually coated with the polymer that constitutes the continuous matrix of the composite [8]. Good dispersion also allows for a more uniform stress distribution and minimizes the appearance of stress-concentration points. A random orientation of fibrous composites results in lower efficiency of reinforcement than does perfect alignment, but perfect alignment generates anisotropy in the mechanical properties. The alignment is necessary when maximization of the strength and modulus are needed in particular directions [9].

Electrospinning has been explored as an efficient process for obtaining nanofibres with diameters in the submicrometre range [10]. The interesting properties of electrospun fibres include increased surface-area-to-volume ratio as a consequence of the diameter, and the high interconnectivity and porosity of the nanofibre meshes at the micrometre length scale [11]. Another inherent feature of the electrospun nanofibres is their ability to mimic the ECM of a variety of tissues, which can create a more favourable microenvironment for the cells [12]. Thus, their use in tissue/organ repair and regeneration as biocompatible and biodegradable medical implant devices has been suggested by many authors [13–15]. The nanoscale size of the biodegradable fibres may also offer advantages in inducing a specific kinetics of degradation. Different nanofibrous structures have already been produced by this technology using a number of both natural and synthetic polymers, such as collagen [16], chitosan [17], silk fibroin [12] and polycaprolactone [18] or polylactides [19]. An important disadvantage of collagen, gelatine, keratin and elastin is their animal origin, remaining a concern in relation to immunogenicity and disease transmission [20]. The present work uses biomaterials from a marine source as an alternative. Chitin is a biopolymer found in nature and is derived mainly from the exoskeletons of crustaceans, insects and molluscs, and the cell wall of micro-organisms. Chitin is a glucose-based polysaccharide. Chitosan is an alkaline deacetylated derivative of chitin. This material is a polysaccharide and shares some structural similarities with glycosaminoglycans. Chitosan is non-cytoxic, biodegradable and reported as potentially biocompatible [21].

Composite materials using synthetic and natural-based materials are increasingly proposed for biomedical applications [22–24]. The chronic inflammatory responses and cytoxicity of some synthetic polymers are reduced or eliminated by the composition with natural polymers. Natural polymers such as chitosan [25], collagen [6], soy [20], alginate [26], silk [12] or starch [27] have already been proposed in many biomedical applications. The biological environment is prepared to recognize these biopolymers and to interact with them metabolically. Another attractive feature of natural polymers is their ability to be cleaved by naturally occurring enzymes, facilitating degradation by physiological mechanisms [28].

Synthetic biodegradable polymers are already used extensively in the biomaterials field including biodegradable aliphatic polyesters, such as poly(lactic acid), poly(glycolic acid) or poly(caprolactone) and its copolymers. Most synthetic polymers are degraded via hydrolysis. The polyester bonds of synthetic polymers are hydrolysed in nontoxic natural metabolites and are eliminated from the body by the normal physiological processes [29]. Therefore, composite materials using synthetic and natural-based polymer materials are increasingly being developed and designed to improve not only the physical and chemical properties but also to improve biological performance [22,24]. The basis of the composite material in the present work is a microparticulate composite of chitosan microparticles dispersed in poly(butylene succinate) (PBS). This biodegradable material has already been shown to have excellent biological performance both in vitro and in vivo for bone and for cartilage tissue engineering applications [30–33] and tested in various three-dimensional (3D) morphologies. The nanofibres used to reinforce this composite are intended to improve some properties but to preserve the good biological performance already shown.

The aliphatic polyester PBS presents a hydrophobic character. However, the chitosan structure is rich in polar groups ($-OH$ and $-NH_2$). Therefore, its presence in the composite resulted in a significant increase in the hydrophilicity [32]. The microparticulate composites (with particles of chitosan) have thus enhanced the hydrophilic properties, thus resulting in a higher variation in mass and tensile modulus, as was confirmed after degradation tests [34]. The kinetics of loss of tensile modulus after degradation can be modulated by the introduction of nanofibres in the particulate composite. The fibrous reinforcement provides additional elastic modulus but also enhances the surface-area-to-volume ratio, facilitating access of water to the

chitosan phase and causing an increase in the water uptake capability of the particulate composite.

Several polymer processing methods have been proposed for producing porous scaffolds that can mimic the architecture of the natural ECM, including freeze drying [35], particle leaching [24], rapid prototyping [36], fibre bonding [37], injection moulding [38] and electrospinning [39]. The composite produced in this work aims to develop 3D porous structures for tissue engineering using a fibre bonding technique.

This work reports the development of a novel particulate composite reinforced with chitosan nanofibre meshes obtained by electrospinning according to Scheme 1. This composite is intended to enhance the mechanical properties and the degradation kinetics of the microfibres, but not to affect negatively the good biological performance of the combination of PBS with chitosan microparticles already demonstrated. Thus, a modest quantity of chitosan nanofibre mesh reinforcement (0.05 wt.%) was used in the microfibres. The morphology, mechanical properties and degradation kinetics were analysed after various periods of immersion in an isotonic saline solution (ISS) of the novel composites intended for tissue engineering scaffolding.

2. Materials and methods

2.1. Materials

Medium molecular weight chitosan was supplied by France Chitin (Orange, France), with a degree of deacetylation of ∼85%. PBS Bionolle 1050 was supplied by Showa Highpolymer Co. Ltd. (Tokyo, Japan). Trifluoroacetic acid (TFA) was obtained from Sigma, and dichloromethane (MC) was supplied by Aldrich. Ammonia 7N solution in methyl alcohol was purchased from Aldrich, methanol was obtained from Fluka, and both were used as neutralizing agents.

2.2. Preparation of chitosan nanofibre meshes

The preparation of a 6 wt.% chitosan solution follows a protocol detailed elsewhere [17], with minimal modifications. In short, the polymer powder was added to a solution containing both TCS and MC, in a volume ratio of 70:30. Before processing, the solution was left under stirring overnight at room temperature. Electrospinning was used to obtain chitosan nanofibre meshes; the polymer solution was placed into a 5 ml syringe with a capillary attached to it. The circular orifice of the capillary had an internal diameter of 0.8 mm. The syringe was further connected to a syringe pump (KDS100, KD Scientific, USA) to control the flow rate. A positive electrode was put in contact with the metal capillary. Aluminium foil was used as the ground collector. A high voltage power supply was employed to generate the electric field (0–25 kV). The capillary tip-to-collector distance and the flow rate were fixed at 12 cm and 0.8 ml h^{-1}, respectively. The applied voltage was optimized to obtain a continuous deposition in the range 15–20 kV. All the electrospinning experiments were performed at room temperature. The solvent evaporation of the meshes was allowed at room temperature for at least 2 days. The next step was the neutralization of the electrospun chitosan nanofibre meshes to prevent their dissolution in aqueous medium. The process of neutralization was based on the work of Notin et al. [40], with several modifications. A weak basic aqueous solution of ammonia 7N in methyl alcohol and methanol was prepared. After immersion in this solution, the meshes were repeatedly washed with distilled water until neutral pH was obtained. The meshes were further dried in the oven at 60 °C for 2 h.

2.3. Preparation of particulate microfibres by extrusion

Two different types of particulate microfibres were produced in this study (i) a microfibre composed of a particulate composite of chitosan (50 wt.%) and PBS; (ii) a microfibre composed of a particulate composite chitosan/PBS (99.95 wt.%) reinforced with 0.05 wt.% chitosan nanofibre meshes. The particulate composite was previously extruded and milled into a powder using a Retsch mill. The chitosan nanofibre meshes were further added during a second extrusion procedure, which was also performed for the particulate composite without nanofibres. The final particulate microfibres were processed on a vertical, in-house developed, micro-extruder [41]. The processing conditions were optimized to obtain stable extrusion processing. Those conditions were kept constant for both compositions to maintain a constant thermal history. The processing parameters were a melt temperature of 145 °C, a screw rotation speed of 40 rpm and a die diameter of 0.5 mm.

2.4. Morphological analysis

The morphology of particulate microfibre composites (with and without nanofibre mesh reinforcements) was analysed by scanning electron microscopy (SEM) (model S360, Leica Cambridge) after being sputter coated with gold. To analyse the distribution, structure, morphology and alignment of the chitosan nanofibres inside the partic-
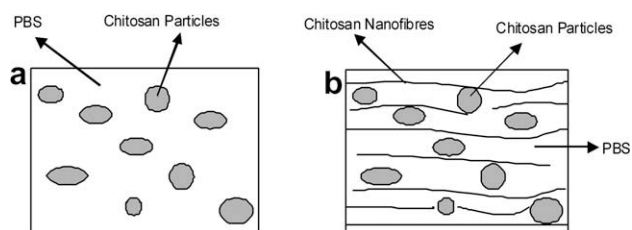
Scheme 1. Representation of the particulate composites: (a) PBS matrix reinforced with chitosan particles – particulate microfibres; (b) PBS matrix reinforced by chitosan particles and nanofibre meshes – particulate microfibres reinforced by nanofibres.

ulate microfibres, a partial dissolution of the polyester matrix with MC was performed at the microfibre surface.

2.5. Mechanical tests

Samples from the two different particulate microfibre compositions were subjected to tensile tests to evaluate the effect of the reinforcement with chitosan nanofibre meshes over the mechanical properties. Samples were also subjected to degradation tests, after which mechanical tests were performed to characterize the evolution of the mechanical properties (tests were performed in the dry state). The particulate microfibres were cut to obtain 10-mm-long fibre specimens ∼500 μm in diameter. The tensile strength was taken as the maximum stress of the stress–strain curve. The tensile modulus was evaluated using the maximum slope of the stress–strain curve. The tensile tests were performed at room temperature in a Universal Mechanical Test Machine (Instron 4505) using a load cell of 2.5 N and a crosshead speed of 5 mm min^{-1}. A minimum of five specimens were tested in each sample (the values reported are the average of those results).

2.6. Swelling and degradation-related tests

The hydration degree and degradation behaviour of the particulate microfibre compositions were assessed over a period of 30 days. Five specimens of each sample (previously weighed) were immersed in an ISS (0.154 M NaCl aqueous solution, pH 7.4) for 1, 3, 7, 14 and 30 days. After each defined period of time, the specimens were removed from the ISS, and the weight was measured. The water uptake was calculated by the following expression:

$$\text{Water uptake}(\%) = [(m_t - m_0)/m_0] \times 100 \qquad (1)$$

where m_0 is the initial weight of the specimen before immersion and m_t is the wet mass of the specimen at time t (days) after being removed from the solution, washed with distilled water, and gently blotted with a paper filter and immediately weighed.

The amount of degradation was calculated using the following expression:

$$\text{Weight loss}(\%) = [(m_{f,t} - m_0)/m_0] \times 100 \qquad (2)$$

where $m_{f,t}$ is the final mass after immersion and drying of the specimen at 60 °C until equilibrium (constant weight) is reached and m_0 is the initial weight of the specimen before immersion. The surfaces of the samples subjected to degradation tests were analysed by SEM to evaluate the surface erosion and the resulting porous morphology.

3. Results and discussion

3.1. Morphological analysis

Fig. 1a presents the morphology of chitosan nanofibre meshes obtained by the electrospinning process (after being subjected to neutralization treatment). The images show that the initial morphology of the nanofibres is preserved after the neutralization process. The nanofibrous mesh obtained consists of fibres with diameters ranging from 65 nm to 6 μm, with interconnected pores in a non-woven structure. Furthermore, the nanofibres present a solid surface, with regular and smooth topography. It was also observed that the fibres do not have beads that are considered a typical problem of electrospun nanofibres [42]. This regular morphology shows the effectiveness of the optimized conditions used in the electrospinning and neutralization processes.

Fig. 1b shows the SEM micrographs of the produced particulate microfibres (without nanofibre mesh reinforcements) obtained by extrusion. The particulate microfibres have average diameter of ∼500 μm. The particulate microfibres seem to be structured in its main axis and oriented due to the extrusion process. The production conditions were optimized to obtain microfibres in a continuous and stable operation. The particulate microfibres are characterized by an irregular surface topography, caused by the presence of the large chitosan particles. The surface of the particulate microfibre is composed almost totally of polyester that is the continuous phase, with the chitosan particles in the inner regions of the fibres. This is caused by the fact that the chitosan particles do not melt [22].

Fig. 1c shows a particulate microfibre reinforced by chitosan nanofibre meshes (0.05 wt.%), where it is possible to observe nanofibres underneath and occasionally next to the surface. The particulate microfibres have an average diameter ∼500 μm. This novel composite combines microparticulate composite with chitosan nanofibres (Fig. 1a and b). The nanofibres, although obtained in random meshes, appear with an aligned morphology inside the microfibres (Fig. 2). This novel alignment is probably caused by the hydrodynamics of the flowing melt in the extrusion process [43]. Apparently, defined areas of the particulate microfibre structure show a considerable alignment of chitosan nanofibre reinforcements. In fact, this effect can be observed both in longitudinal and in cross-section micrographs (Fig. 2a and c, respectively). Those SEM analyses were performed in samples in which PBS was dissolved with MC to allow the nanofibres to be identified. The distribution of the nanofibres by volume is adequate, and the adhesion between the matrix and the nanofibres is good, as no voids or spaces close to the interface are observed. In Fig. 2c, it is possible to observe the cross-section of the reinforced microfibre. The image shows the alignment of the nanofibres with the main axis of the particulate microfibre and the intimate coverage of the chitosan nanofibres by the polymer matrix (at the bottom of the micrograph, where the MC has not dissolved the PBS) provided by the melting process. Similar observations are possible in a longitudinal section of the particulate microfibre (Fig. 2b). The alignment of chitosan nanofibres in the matrix suggests that anisotropy of mechanical properties will be present in the particulate microfibres.
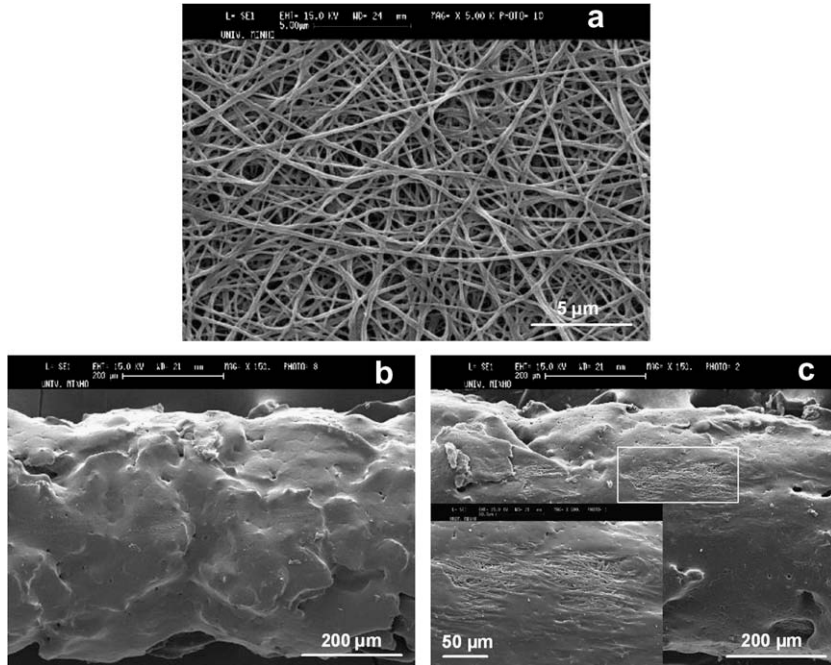
Fig. 1. SEM micrographs of: (a) electrospun chitosan nanofibre meshes; (b) particulate microfibre (without nanofibres); (c) particulate microfibre reinforced by chitosan nanofibre meshes.
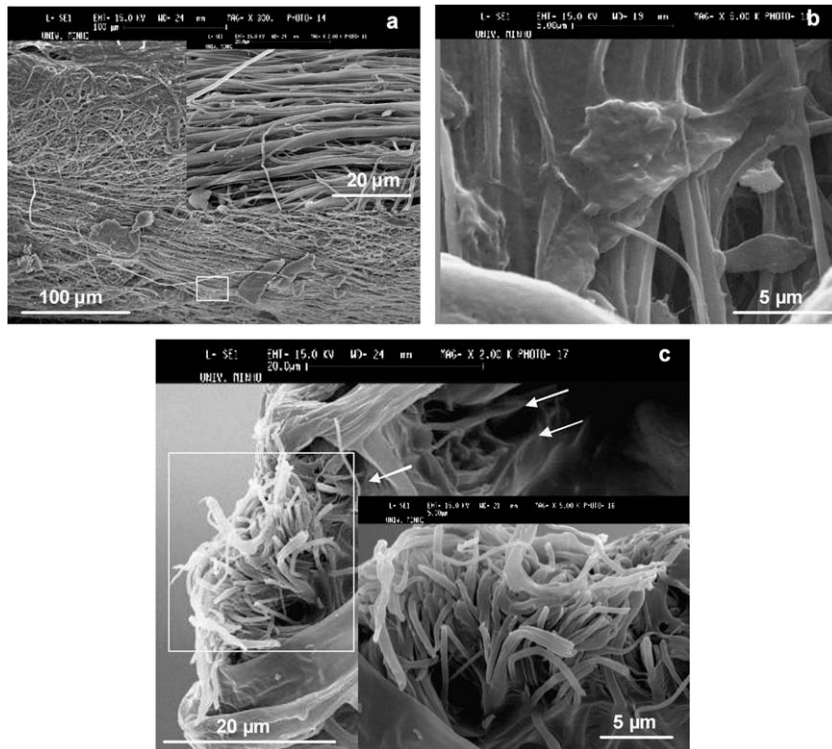

Fig. 2. SEM micrographs of particulate microfibre reinforced by chitosan nanofibre meshes: (a) and (b) longitudinal section; (c) cross-section. In observations, the use of MC was required in order to identify and view nanofibres.

3.2. Mechanical tests

The tensile modulus, tensile stress and tensile strain are all shown in Fig. 3b. A value of 6.20 MPa was obtained for the tensile stress of the unreinforced particulate microfibres and 10.6% for the tensile strain. Particulate microfibres reinforced with chitosan nanofibre meshes shown a tensile stress and strain of 6.9 MPa and 7.9%, respectively. The
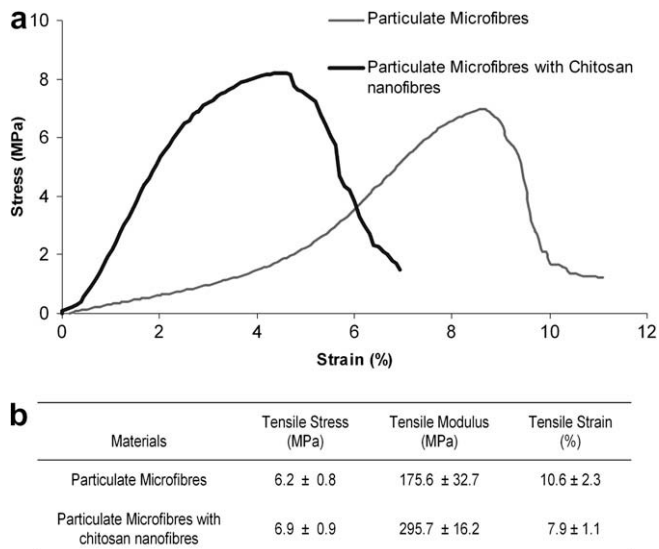
Fig. 3. (a) Representative tensile stress–strain curves of particulate microfibres with and without chitosan nanofibre meshes reinforcements. (b) The mechanical properties obtained from the tensile curves are summarized below the graph.

differences between the tensile stresses of both composites (maximum stress obtained in the tensile test experiment) are not significant, and this has been shown to be the case for many fibre-reinforced composites. In fact, the tensile stress is a property that is strongly connected with the probability of having critical size defects in the material structure. Reinforcement with the nanofibres is shown not to affect this property negatively, this observation being an interesting result. The tensile strain (the maximum strain before breaking of the specimen) is also sensitive to the frequency of defects and its size, but also to the properties of the constituents of the composite. In fact, the two main modes of failure of materials are by reaching the strain limit of the material or by stress concentration at defects. Thus, a decrease in the tensile strain is showing that the material is more brittle, which may be a sign of larger defect sizes developing earlier, or that the material has a lower strain limit associated with the stiffening of the material. The first hypothesis is not confirmed by the results of tensile stress; thus, the more probable cause is that the stiffening of the nanofibre reinforced a lower strain limit in the particulate microfibre composite. This result is also an indication of strong reinforcement of the particulate microfibres by the presence of the nanofibres, as it is typical for a decrease in tensile strain to be associated with effective fibre reinforcements [44].

The particulate microfibres without reinforcement have a tensile modulus of 175.6 MPa. The composition and reinforcement with chitosan nanofibre meshes (0.05 wt.%) caused the tensile modulus to increase by 70% (295.7 MPa). The reinforcement in the main axis of orientation of the nanofibres inside the particulate microfibres probably causes anisotropy, as the properties in directions transversal to the alignment are probably similar to the

properties of the matrix. Generally, the level of anisotropy of the mechanical properties is directly proportional to the efficiency of reinforcement in fibre-reinforced composites. A high level of alignment is necessary to maximize the elastic modulus of the composite, but it is not always favourable. The level of anisotropy in mechanical properties may need to be avoided in 2D or 3D geometries. In fibres, however, the alignment has minimal downside, and it is a good way to maximize the efficiency of reinforcement [8]. In addition, the use of continuous fibre composites is traditionally more effective in achieving improvement in properties. Tensile, flexural and impact properties are significantly enhanced by those reinforcements more than by similar compositions with short fibres [45].

Nanofibre reinforcements with 1 wt.% carbon nanotubes (CNT) in polypropylene were shown to result in a 60% increase in the elastic modulus [46]. Other studies with composites of polypropylene reinforced by 5 wt.% single wall CNT resulted in a 350% larger elastic modulus [47] when compared with the properties of the matrix. Those studies inspired the work presented in the present paper.

In this study, a novel micro–nano composite was developed by producing microfibres of a natural-synthetic polymeric particulate composite reinforced with nanofibres from a natural polysaccharide. The elastic modulus of the particulate composite was significantly enhanced, even with a low content of nanofibre reinforcement.

Fig. 3a shows a representative stress–strain curve of the particulate microfibre composite specimens. The evolution of stress with strain follows a similar trend of variation in qualitative terms, the only noticeable difference being in the strain capacity after the tensile stress peak is reached. The particulate composite failed rapidly after the maximum stress, while the reinforced particulate microfibres showed some strain capacity after reaching the maximum stress. The tensile stress in the nanofibre-reinforced particulate composite is more efficiently transferred to the nanofibres, enabling some additional plastic strain to be obtained.

A non-uniform dispersion may lead to local agglomeration of nanofibres within the matrix. Thus, the bulk material has two types of interface, namely the nanofibre–matrix and the particle–matrix interfaces. The interfacial shear strength between the nanofibres and matrix may be excellent, but the interfacial shear strength in particulate composites is frequently not ideal, owing to not only geometrical considerations but also to the difficulty in dispersing the particles well. The fact that the nanofibres are longer and well oriented means that more surface area is provided to develop a good interface with the matrix. As a result, not only the stiffness, but also the tensile strength of the particulate microfibres reinforced with chitosan nanofibres increased (Fig. 3a) when compared with the unreinforced particulate composite. The tensile strength of a particulate composite is dependent mainly on the tensile strength of the matrix and on the number and size of local defects. The properties of the interface are also very

important for ensuring the load transfer process and thus increasing the reinforcing efficiency [22].

It can be said that the elastic modulus of the microfibres, a particulate composite, is significantly improved when it is reinforced by chitosan nanofibres (0.05 wt.%). The tensile strength is marginally improved, and the tensile strain is reduced considerably, as is typical for fibre-reinforced composites.

3.3. Swelling and degradation tests

Water uptake is an important aspect of the characterization of biodegradable polymers intended for biomedical applications. It is also useful to evaluate the degree of swelling and obtain information about the hydrophilic/hydrophobic character of the materials in immersion conditions. Indeed, the rate of water uptake depends on various physical and chemical properties such as hydrophilicity, crystallinity and surface area [34].

Fig. 4a shows very large water absorption in chitosan nanofibre meshes, with maximum water uptake after 7 days of immersion (up to 300%). Both the surface-area-to-volume ratio and the chitosan hydrophilicity contribute to increasing the water uptake capability of the composite. The neutralization process was efficiently performed, as nanofibres do not dissolve on immersion in ISS. The structure of the fibres was preserved, and the swelling was significantly enhanced. Even after 30 days of immersion in ISS, the nanofibre morphology remained stable and swollen, as is clearly shown in Fig. 5f–h.

The equilibrium water uptake in particulate microfibres both with and without chitosan nanofibres was already reached at the end of the first day. The differences in water uptake caused by the chitosan nanofibre reinforcements are significant. The particulate composite microfibres reached a maximum of 16% of water uptake on the third day (Fig. 4a). The introduction of chitosan nanofibres increased the water uptake to 24%, reaching a maximum

on day 15. Despite the low amount of chitosan nanofibre meshes (0.05 wt.%), a significant increment of water absorption was observed in the particulate composite. These results are related to the high surface area of the nanofibres, facilitating the intake of water and the properties of chitosan, a very hydrophilic natural polymer. In addition, the chitosan nanofibres are present underneath the surface of the particulate microfibres, enhancing the opportunities for water diffusion into the chitosan phase of the composite (Fig. 1c).

The initial diameter of the particulate microfibres without and with nanofibres was 500 μm and after being subjected to water uptake tests, the diameter of the particulate microfibres increased (ability to swell). After 30 days of immersion, the particulate microfibres without reinforcement showed diameters of 556 ± 3.2 μm, and the particulate microfibres reinforced by chitosan nanofibres showed diameters of 571 ± 4.1 μm, thus confirming the swelling of the composite.

The degradation rate of the material depends on its crystallinity, molecular weight and susceptibility to hydrolysis. The limit value for the water uptake should be regarded as a result of two complementary phenomena: the intrinsic water uptake capability of the material; and the degradation history. Those phenomena are somewhat interrelated, as higher water absorption usually accelerates the degradation process, particularly in materials sensitive to hydrolysis [48]. This is the main reason why the water uptake should be complemented and analysed together with the weight loss data [34]. In this study, the degradation of particulate microfibres was analysed by the changes in their physicochemical properties (weight loss and tensile properties).

Fig. 4b shows the weight loss results of the studied structures: particulate microfibres with or without chitosan nanofibre meshes. Data are also provided on the behaviour of chitosan nanofibre meshes. Chitosan nanofibres showed a maximum weight loss of 33% after 30 days of immersion in ISS. The small fibre diameter (leading to higher surface
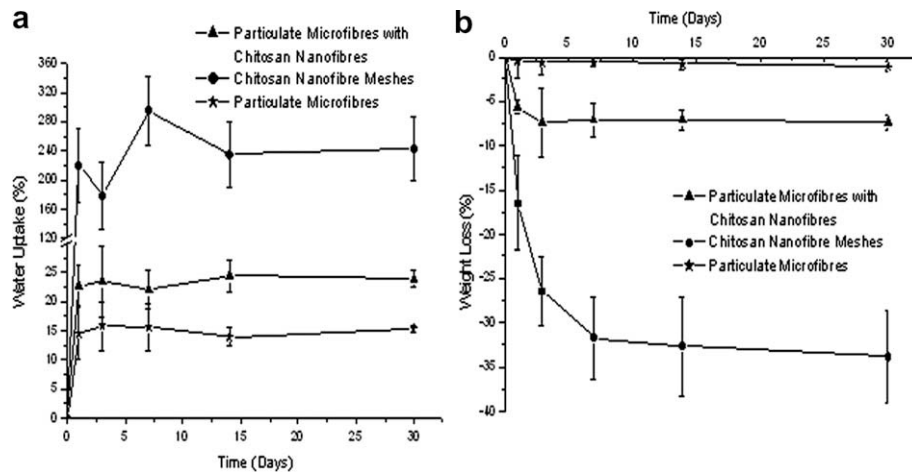

Fig. 4. (a) Percentage water uptake against experimental time course. (b) Percentage weight loss against different degradation times of particulate microfibres reinforced by chitosan nanofibre meshes, chitosan nanofibre meshes and particulate microfibres (without nanofibres).
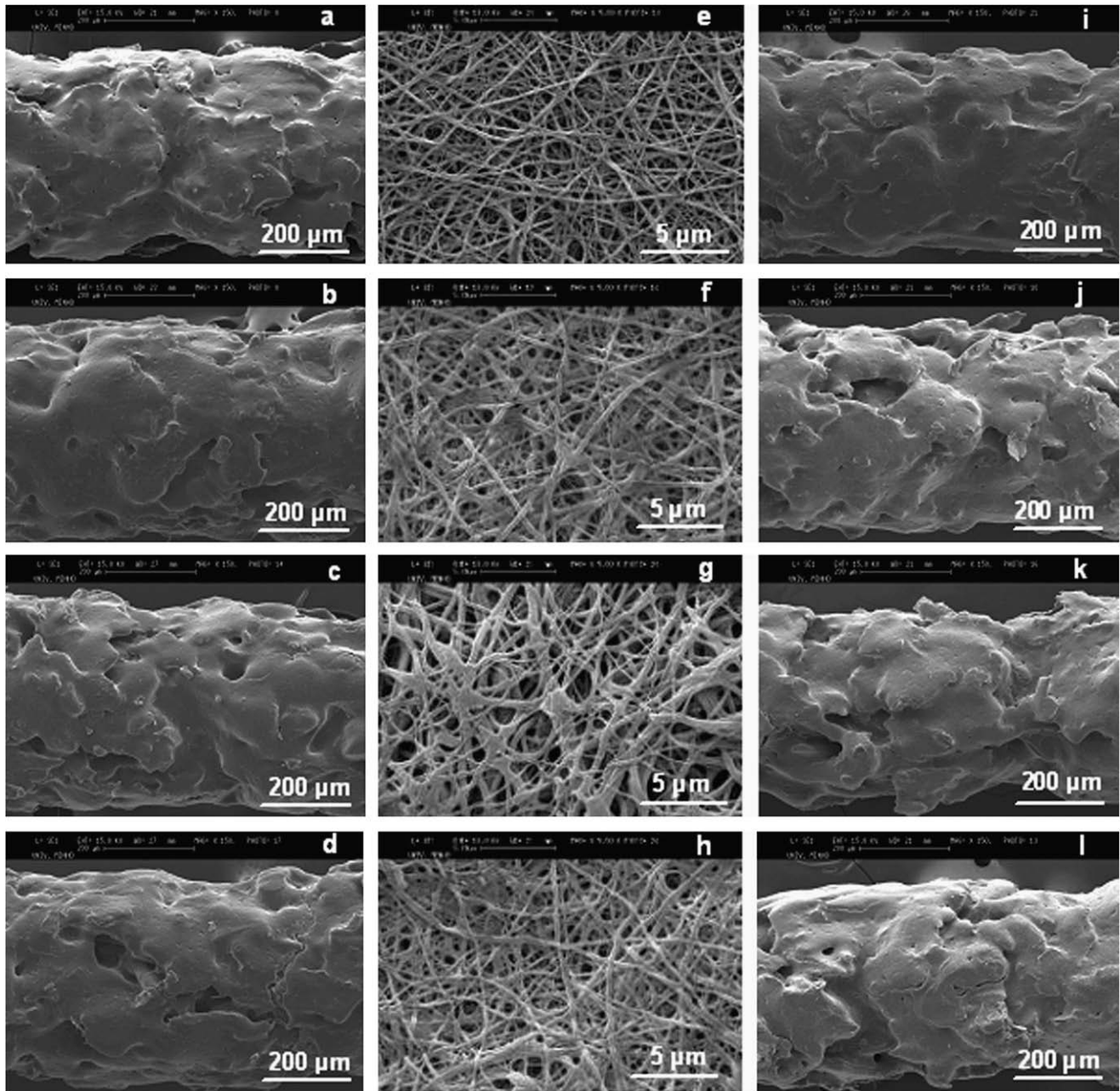
Fig. 5. SEM micrographs of the surface topography of (b–d) particulate microfibres (without reinforcement), (f–h) chitosan nanofibre meshes and (j–l) particulate microfibres reinforced with chitosan nanofibre meshes, submitted to degradation tests: (a, e, i) samples not subjected to degradation tests; samples after immersion in ISS, for different time periods of degradation: (b, f, j) 7 days; (c, g, k) 14 days and (d, h, l) 30 days.

area and hydrophilic nature) results in faster degradation of the chitosan nanofibres [18]. Fig. 5e–h illustrates the surface morphological changes in chitosan nanofibres during the periods of immersion. After 1 day of immersion, the chitosan nanofibres were considerably swollen, and an increase in the surface roughness was observed. Additionally, most fibres were partially adhered, causing a more compact mesh structure after 30 days of immersion (Fig. 5h).

The weight loss of the particulate microfibres without nanofibre reinforcement reached a maximum value of 1% after being subjected to 30 days of immersion tests. Although the particulate microfibres show low values of weight loss, some erosion and development of surface porosity is observed (Fig. 5b–d). The presence of the chitosan particles is causing local swelling and opening the outer skin layer of the polymer matrix. In the case for particulate microfibres reinforced by chitosan nanofibres, the weight loss reached a maximum of 7.4% after the third day of immersion. This increment of weight loss is a direct consequence of the introduction of chitosan nanofibres into the particulate microfibre structure. Similarly to the behaviour

of water uptake, the weight loss increases in particulate microfibres reinforced with nanofibre meshes. Fig. 5i–l shows the surface topography of the particulate microfibres reinforced by chitosan nanofibres before and after immersion in ISS. The surface shows local porosity probably caused by the partial erosion of the inner chitosan particles and nanofibres. The presence of chitosan nanofibres causes more hydrophilic behaviour of the particulate microfibres, and enhances the mechanisms of erosion and degradation of the chitosan phase, consequently also facilitating the hydrolysis of the PBS matrix, resulting in faster degradation of the composite.

The mechanical properties of the particulate microfibres after the degradation tests decrease, as expected (Fig. 6). A slight decrease in the modulus at longer immersion periods can be explained by the erosion of the chitosan phase. The elongation values did not increase in the case of microfibres without nanofibre reinforcement (Fig. 6b). However, the ultimate tensile strain values decreased owing to the erosion and degradation of chitosan particles and by an enhancement of the critical size defects in the structure of the unreinforced particulate microfibres. For the particulate microfibres reinforced with chitosan nanofibres, the modulus also decreases with time of immersion, but consistently presents a higher modulus when compared with the particulate microfibres for similar periods of immersion.

The tensile modulus of particulate microfibres reinforced by chitosan nanofibres after 30 days of degradation tests (Fig. 6c) was higher than the unreinforced particulate microfibres before being subjected to immersion tests— their initial tensile modulus properties (Fig. 3b).

The variation in the tensile strength values is not as significant as the variation in the tensile modulus, and particulate microfibres with and without nanofibres present similar values after being subjected to 30 days of degradation tests (Fig. 6c).

In Fig. 6a, the particulate microfibres composite reinforced with chitosan nanofibres did not present significant changes in the ultimate tensile strain values. Here, the degradation kinetics increased and the mechanical properties, after being subjected to immersion tests, were maintained at higher values when compared with unreinforced particulate microfibres.

4. Conclusions

This work focused on the development of new particulate microfibre composites. The particulate microfibres have a synthetic polymeric matrix, were reinforced by chitosan particles and were studied with and without chitosan nanofibre mesh reinforcements. The nanofibres although being initially obtained in randomly aligned
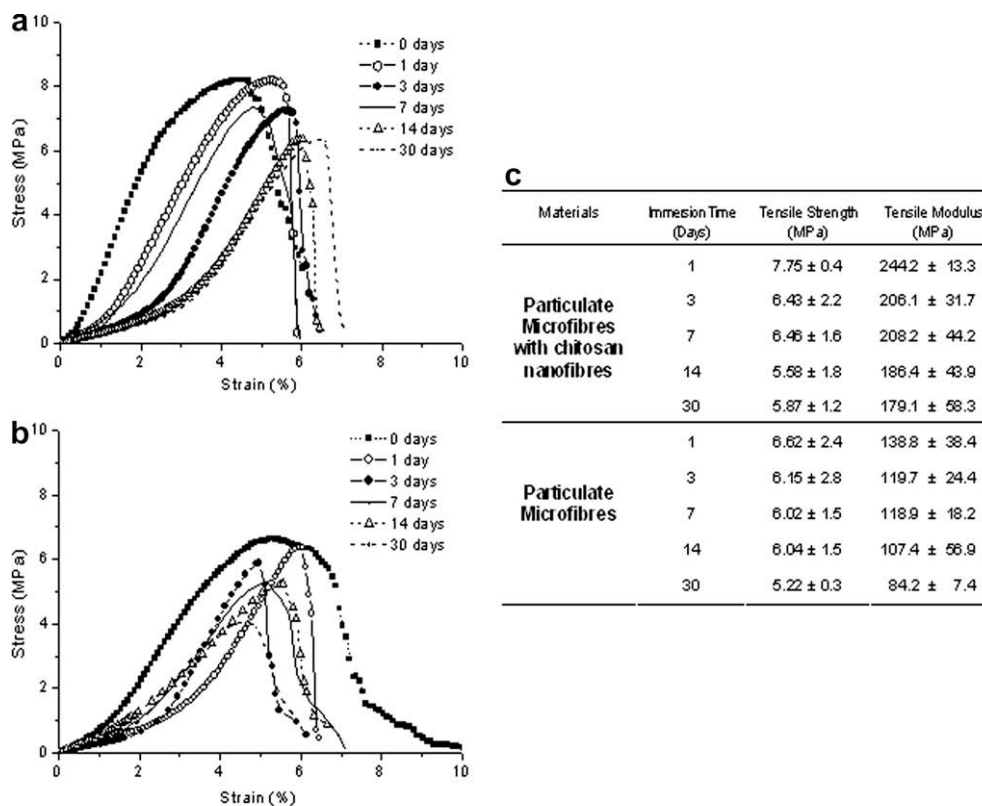

Materials	Immersion Time (Days)	Tensile Strength (MPa)	Tensile Modulus (MPa)
Particulate Microfibres with chitosan nanofibres	1	7.75 ± 0.4	244.2 ± 13.3
	3	6.43 ± 2.2	206.1 ± 31.7
	7	6.46 ± 1.6	208.2 ± 44.2
	14	5.58 ± 1.8	186.4 ± 43.9
	30	5.87 ± 1.2	179.1 ± 58.3
Particulate Microfibres	1	6.62 ± 2.4	138.8 ± 38.4
	3	6.15 ± 2.8	119.7 ± 24.4
	7	6.02 ± 1.5	118.9 ± 18.2
	14	6.04 ± 1.5	107.4 ± 56.9
	30	5.22 ± 0.3	84.2 ± 7.4

Fig. 6. Representative tensile stress–strain curves of particulate microfibres after been subjected to swelling and degradation tests: (a) reinforced by chitosan nanofibre meshes; (b) without nanofibre reinforcements; (c) on the side of the graphs are summarized the tensile strength and modulus obtained from the stress–strain curves.

meshes, appeared with a well-aligned morphology inside the particulate microfibres. The longitudinal and cross-sections of the nanofibre-reinforced particulate microfibres showed considerable alignment of the chitosan nanofibres along the longitudinal axis of the microfibres caused by the melt flow during extrusion.

Mechanical tests showed that the nanofibre reinforcement in the particulate microfibre composite significantly increased (70%) the tensile modulus. This tensile modulus enhancement was obtained with only 0.05 wt.% of chitosan nanofibre meshes.

The chitosan nanofibre reinforcement in the particulate microfibres increased the water uptake by up to 24%. The weight loss also increased, indicating that the kinetics of biodegradation was significantly accelerated by the presence of the nanofibre reinforcement.

The tensile modulus of particulate microfibres reinforced by chitosan nanofibres after 30 days of degradation tests, despite having a weight loss of 7%, was still larger than the unreinforced particulate microfibres before being subjected to the degradation experiments.

The new particulate microfibre composite has enhanced mechanical and degradation properties and represents a new strategy for designing materials with properties tailored for many biomedical applications.

Acknowledgements

References

[1] Provenzano PP, Vanderby Jr R. Collagen fibril morphology and organization: implications for force transmission in ligament and tendon. Matrix Biol 2006;25:71–84.

[2] Murugan R, Ramakrishna S. Development of nanocomposites for bone grafting. Comp Sci Technol 2005;65:2385–406.

[3] MacDonald RA, Laurenzi BF, Viswanathan G, Ajayan PM, Stegemann JP. Collagen–carbon nanotube composite materials as scaffolds in tissue engineering. J Biomed Mater Res A 2005;74:489–96.

[4] Lutolf MP, Hubbell JA. Synthetic biomaterials as instructive extracellular microenvironments for morphogenesis in tissue engineering. Nat Biotechnol 2005;23:47–55.

[5] Pins GD, Christiansen DL, Patel R, Silver FH. Self-assembly of collagen fibres: influence of fibrillar alignment and decorin on mechanical properties. Biophys J 1997;73:2164–72.

[6] Lee P, Lin R, Moon J, Lee LP. Microfluidic alignment of collagen fibres for *in vitro* cell culture. Biomed Microdevices 2006;8:35–41.

[7] Kim J-S, Reneker DH. Mechanical properties of composites using ultrafine electrospun fibres. Polym Compos 1999;20:124–31.

[8] Coleman JN, Khan U, Gun'ko YK. Mechanical reinforcement of polymers using carbon nanotubes. Adv Mater 2006;18:689–706.

[9] Liu L-Q, Tasis D, Prato M, Wagner HD. Tensile mechanics of electrospun multiwalled nanotube/poly(methyl methacrylate) nanofibres. Adv Mater 2007;19:1228–33.

[10] Venugopal J, Vadgama P, Kumar TSS, Ramakrishna S. Biocomposite nanofibres and osteoblasts for bone tissue engineering. Nanotechnology 2007;18:511–9.

[11] Lin T, Wang H, Wang X. Self-crimping bicomponent nanofibres electrospun from polyacrylonitrile and elastomeric polyurethane. Adv Mater 2005;17:2699–703.

[12] Li C, Vepari C, Jin H-J, Kim HJ, Kaplan DL. Electrospun silk-BMP-2 scaffolds for bone tissue engineering. Biomaterials 2006;27:3115–24.

[13] Neves NM, Campos R, Pedro A, Cunha J, Macedo F, Reis RL. Patterning of polymer nanofibre meshes by electrospinning for biomedical applications. Int J Nanomed 2007;2:433–48.

[14] Araujo JV, Martins A, Leonor IB, Pinho ED, Reis RL, Neves NM. Surface controlled biomimetic coating of polycaprolactone nanofibre meshes to be used as bone extracellular matrix analogues. J Biomater Sci Polym Ed 2008;19:1261–78.

[15] Yoshimotoa H, Shina YM, Teraia H, Vacanti JP. A biodegradable nanofibre scaffold by electrospinning and its potential for bone tissue engineering. Biomaterials 2003;24:2077–82.

[16] Sefcik LS, Neal RA, Kaszuba SN, Parker AM, Katz AJ, Ogle RC, et al. Collagen nanofibres are a biomimetic substrate for the serum-free osteogenic differentiation of human adipose stem cells. J Tissue Eng Regen Med 2008;2:210–20.

[17] Ohkawa K, Cha D, Kim H, Nishida A, Yamamoto H. Electrospinning of chitosan. Macromol Rapid Commun 2004;25:1600–5.

[18] Chong EJ, Phan TT, Lim IJ, Zhang YZ, Bay BH, Ramakrishna S, et al. Evaluation of electrospun PCL/gelatin nanofibrous scaffold for wound healing and layered dermal reconstitution. Acta Biomater 2007;3:321–30.

[19] Inai R, Kotaki M, Ramakrishna S. Structure and properties of electrospun PLLA single nanofibres. Nanotechnology 2005;16:208–13.

[20] Vaz CM, de Graaf LA, Reis RL, Cunha AM. Soy protein-based systems for different tissue regeneration. In: Reis RL, Cohn D, editors. Polymer based systems on tissue engineering, replacement and regeneration, Nato Science Series. Dordrecht: Kluwer; 2002. p. 93–110.

[21] Rinaudo M. Chitin and chitosan: properties and applications. Prog Polym Sci 2006;31:603–32.

[22] Correlo VM, Boesel LF, Bhattacharya M, Mano JF, Neves NM, Reis RL. Properties of melt processed chitosan and aliphatic polyester blends. Mater Sci Eng A 2005;403:57–68.

[23] Correlo VM, Boesel LF, Bhattacharya M, Mano JF, Neves NM, Reis RL. Hydroxyapatite reinforced chitosan and polyester blends for biomedical applications. Macromol Mater Eng 2005;290:1157–65.

[24] Correlo VM, Boesel LF, Pinho ED, Costa-Pinto AR, Alves da Silva ML, Bhattacharya M, et al. Melt-based compression moulded scaffolds from chitosan-polyester blends and composites: morphology and mechanical properties. J Biomed Mater Res A, in press.

[25] Baran ET, Mano JF, Reis RL. Starch-chitosan hydrogels prepared by reductive alkylation cross-linking. J Mater Sci Mater Med 2004;15:759–65.

[26] Bhattarai N, Li Z, Edmondson D, Zhang M. Alginate-based nanofibrous scaffolds: structural, mechanical, and biological properties. Adv Mater 2006;18:1463–7.

[27] Silva GA, Pedro A, Costa FJ, Neves NM, Coutinho OP, Reis RL. Soluble starch and composite starch bioactive glass 45S5 particles: synthesis, bioactivity, and interaction with rat bone marrow cells. Mater Sci Eng C 2005;25:237–346.

[28] Mano JF, Silva GA, Azevedo HS, Malafaya PB, Sousa RA, Silva SS, et al. Natural origin biodegradable systems in tissue engineering and regenerative medicine: present status and some moving trends. J R Soc Interface 2007;4:999–1030.

[29] Gunatillake PA, Adhikari R. Biodegradable synthetic polymers for tissue engineering. Eur Cells Mater 2003;5:1–16.

[30] Costa-Pinto AR, Salgado AJ, Correlo VM, Sol PC, Bhattacharya M, Charbord P, et al. Adhesion, proliferation and osteogenic differentiation of a mouse mesenchymal stem cell line (BMC9) seeded on

novel melt based chitosan/polyester 3D porous scaffolds. Tissue Eng A 2008;14:1049–57. doi:10.1089/ten.tea.2007.015.

[31] Oliveira JT, Correlo VM, Sol PC, Costa-Pinto AR, Salgado AJ, Bhattacharya M, et al. Assessment of the suitability of chitosan/polybutylene succinate scaffolds seeded with mouse mesenchymal progenitor cells for a cartilage tissue engineering approach. Tissue Eng A 2008:14. doi:10.1089/ten.tea.2007.030 [ahead of print].

[32] Coutinho DF, Pashkuleva I, Alves CM, Marques AP, Neves NM, Reis RL. The effect of chitosan on the in vitro biological performance of chitosan-poly(butylene succinate) blends. Biomacromolecules 2008;9:1139–45.

[33] Mrugala D, Bony C, Neves NM, Caillot N, Fabre S, Moukoko D, et al. Phenotypic and functional characterization of ovine mesenchymal stem cells: application to a cartilage defect model. Ann Rheum Dis 2008;67:288–95.

[34] Correlo VM, Pinho ED, Pashkuleva I, Bhattacharya M, Neves NM, Reis RL. Water absorption and degradation characteristics of chitosan-based polyesters and hydroxyapatite composites. Macromol Biosci 2007;7:354–63.

[35] Song E, Kim SY, Chunc T, Byun H-J, Lee YM. Collagen scaffolds derived from a marine source and their biocompatibility. Biomaterials 2006;27:2951–61.

[36] Woesz A, Rumpler M, Stampfl J, Varga F, Fratzl-Zelman N, Roschger P, et al. Towards bone replacement materials from calcium phosphates via rapid prototyping and ceramic gel casting. Mater Sci Eng C 2005;25:181–6.

[37] Santos MI, Fuchs S, Gomes ME, Unger RE, Reis RL, Kirkpatrick CJ. Response of micro- and macro-vascular endothelial cells to starch-based fiber meshes for bone tissue engineering. Biomaterials 2007;28:240–8.

[38] Neves NM, Kouyumdzhiev A, Reis RL. The morphology, mechanical properties and ageing behaviour of porous injection moulded starch-based blends for tissue engineering scaffolding. Mater Sci Eng C 2005;25:195–200.

[39] Tuzlakoglu K, Bolgen N, Salgado AJ, Gomes ME, Piskin E, Reis RL. Nano- and micro-fiber combined scaffolds: a new architecture for bone tissue engineering. J Mater Sci Mater Med 2005;16:1099–104.

[40] Notin L, Viton C, Lucas J-M, Domard A. Pseudo-dry-spinning of chitosan. Acta Biomater 2006;2:297–311.

[41] Covas JA, Costa P. A miniature extrusion line for small scale processing studies. Polym Test 2004;23:763–73.

[42] Li D, Xia Y. Electrospinning of nanofibres: reinventing the wheel? Adv Mater 2004;16:1151–70.

[43] Neves NM, Isdell G, Pouzada AS, Powell PC. On the effect of the fiber orientation on the flexural stiffness of injection molded short fiber reinforced polycarbonate plates. Polym Compos 1998;19:640–51.

[44] Mahfuza H, Adnana A, Rangaria VK, Jeelania S, Jangb BZ. Carbon nanoparticles/whiskers reinforced composites and their tensile response. Compos A 2004;35:519–27.

[45] Krause W, Henning F, Ster ST, Geiger O, Eyerer P. LFT-D—a process technology for large scale production of fiber reinforced thermoplastic components. J Thermoplast Compos Mater 2003;16:280–302.

[46] Moore EM, Ortiz DL, Marla VT, Shambaugh RL, Grady BP. Enhancing the strength of polypropylene fibres with carbon nanotubes. J Appl Polym Sci 2004;93:2926–33.

[47] Changa TE, Jensenb LR, Kisliuka A, Pipesc RB, Pyrzb R, Sokolov AP. Microscopic mechanism of reinforcement in single-wall carbon nanotube/polypropylene nanocomposite. Polymer 2005;46:439–44.

[48] Pavlov MP, Mano JF, Neves NM, Reis RL. Production and characterization of fibres and 3D mesh scaffolds from biodegradable starch-based blends. Macromol Biosci 2004;4:776–84.